Arabian Journal of Chemistry (2010) **3**, 13–19

King Saud University

Arabian Journal of Chemistry

www.ksu.edu.sa
www.sciencedirect.com

ORIGINAL ARTICLE

Design of molecular precursors for nanomaterials

Taimur Athar

Organic-III, Indian Institute of Chemical Technology, Tarnaka, Hyderabad 500-007, AP, India

Received 16 August 2009; accepted 31 October 2009
Available online 23 December 2009

KEYWORDS

Chemical synthesis;
Bimetallic oxide;
Non-hydrolytic sol–gel process

Abstract This work is focused on the synthesis of bimetallic oxide prepared by non-hydrolytic sol–gel method using the chemie douce approach. The bimetallic oxide was characterized by using various analytical techniques. Elemental analysis showed consistency with the formulation. From XRD, SEM and TEM studies, it is concluded that precursor chemistry has a significant effects on the surface chemistry of metal oxide on calcinations and as well as synthetic routes. XRD patterns show that an enhanced homogeneity on calcinations. Use of these metal oxides has commercial importance in future for sensor devices.

1. Introduction

Understanding and manipulating nanosized particles is an active research area. The family of nanomaterials and their synthesis is a challenge to material scientists due to their fascinating size dependent properties which have distinct properties from their corresponding bulk counterparts as well as from the atomic or molecular precursors from which they are derived.

Modern technologies in nanoage require new materials to improve our life span and style. Metal alkoxides are considered to be best precursor due to the soft reaction conditions with their better compositional uniformity in the final oxides. Metal alkoxides have attracted much attention due to their solubility in a wide variety of organic solvents and their ability to form heterometallic oxides species (Mehrotra, 1992; Brinker et al., 1984; Trevor and Sakka, 2004; Bradley et al., 1978; Turova et al., 2002; Bradley et al., 2001). Alkoxides that display the highest nuclearity are often non-volatile and non-soluble when compared to other alkoxides with low nuclearity. The M–O–C bond polarity and the polymerization mainly govern their solubility, volatility and thermal stability for the design of functional nanomaterials (Bradley et al., 1978; Turova et al., 2002; Bradley et al., 2001).

To protect the green house effect for our modern lifestyle, it is necessary to protect our self with the help of nanodevices such as sensors (electronic, biological) and nanodrug delivery systems in cost-effective techniques. Scientists are trying their best to improve the synthetic techniques in an environmental friendly approach. The role of precursor plays an important role for the synthesis of nanomaterials with controlled particle size and its distribution with a favorable surface morphology. The favorable particle chemistry can be achieved with the help of cost-effective soft chemistry approach (Klabunde, 2000; Sapra and Sarma, 2004; Jolivet, 2000).

In this study the synthesis of heterometallic precursors was carried out to design nanopowder with favorable surface chemistries via wet chemical routes. As we know the chemical reactivity of metal alkoxides towards nucleophilic reactions

E-mail address: taimurathar2001@gmail.com

1878-5352 Peer-review under responsibility of King Saud University.
doi:10.1016/j.arabjc.2009.12.003

Production and hosting by Elsevier

depends largely on the electrophilic character of the metal ion and its ability to increase the coordination number. The coordination unsaturation is the main driving force behind the reactivity of metal alkoxides. A metal oxide has emerged as promising engineering materials due to their ultra pure nature to evaluate the functional properties for new potential applications in sensor devices.

2. Experimental

All manipulations were performed under dry argon using Schlenk line techniques. Solvents and alcohols were purified by standard methods and stored over molecular sieves. FT-IR spectra were recorded from Nujol mulls on a Perkin–Elmer Paragon 500 FT-IR spectrometer. UV–visible spectra were recorded on a unicam UV2-100 spectrometer. The C and H analyses were carried out by using an EA 1110 (CE instrument) elemental analyzer. Ti, Sn, Sb and Ce were determined quantitatively as metal oxide (Vogel, 1989). Isopropoxy content was estimated by the oxidotitration method using standard chromic acid (Mehrotra, 1954). ^{1}H NMR spectra were recorded in $CDCl_3$ or C_6D_6 on a Bruker DRX–300 MHz spectrometer. Mass studies were recorded for fragmentation on a JMS-DX 303 spectrometer. Powder X-ray diffraction measurements were performed at room temperature on D8-Discover (with GADDS) Bruker operating with Cu $K\alpha_1$ radiation. The powder morphology of the compounds before and after heat treatment was investigated using a scanning electron microscope (SEM) Philips XL30S FEG XL V.5.50. Thermal analysis was performed on a TA Instruments SDT960 in a nitrogen atmosphere. The compounds were heated in nitrogen at a rate of 5 °C/min. The experiments were performed in Quartz crucibles, which also served as the reference.

2.1. Synthesis of bimetallic alkoxides

The best controllable and forward route for the preparation of bimetallic alkoxides was carried out under dry N_2 atmosphere in oven-dried glass wares based on the concept of single source precursor (Kessler, 2003; Backov, 2006).

$$K + Pr^iOH \rightarrow KOPr^i + \frac{1}{2}H_2 \uparrow \quad (1)$$

$$KOPr^i + Sb(OPr^i)_3 \rightarrow KSb(OPr^i)_4 \quad (2)$$

$$CeCl_3 + 3KSb(OPr^i)_4 \rightarrow [Ce\{Sb(OPr^i)_4\}_3] + 3KCl \downarrow \quad (3)$$

One equivalent of potassium (0.46 g, 11.76 mmol) reacted with isopropyl alcohol (10 ml) and the resulting reaction mixture was allowed to stir at room temperature for 20 min. The reaction content was then refluxed for 1 h and on cooling addition of one equivalent of freshly distilled antimony isopropoxide (3.41 g, 11.76 mmol) to the same content was made. The mixture was refluxed for 3 h then cooled. One-third equivalent of anhydrous cerium trichloride (0.97 g, 3.92 mmol) was added. Content was stirred and refluxed under nitrogen atmosphere for 12 h. KCl was obtained in quantitative yield and the filtrate was evaporated and the white solid compound was obtained quantitatively was further purified by recrystallization from the mixture benzene–isopropanol. The same procedure was used for the synthesis of bimetallic alkoxides as listed in Table 1.

2.2. Synthesis of mixed oxide derivatives

Four equivalents of anhydrous cerium trichloride (0.812 g, 3.29 mmol) was mixed with one equivalent of $[Ce\{Sb(OPr^i)_4\}_3]$ (1 g, 0.82 mmol) in an anhydrous dichloromethane at room temperature. The resulting reaction mixture was then refluxed with stirring for 36 h in the presence of catalytic amounts of ferric chloride 0.01% (0.0005 g, 0.03 mmol). The mixture was then filtered off and the precipitates were washed several times with anhydrous dichloromethane and dry benzene. White insoluble powder was obtained in a quantitative yield after drying under vacuum for 4 h. The reaction is shown in the following equation:

$$4CeCl_3 + [Ce\{Sb(OPr^i)_4\}_3] \rightarrow [Ce_5Sb_3O_{12}] + 12Pr^iCl \quad (4)$$

The same procedure was used to synthesize other bimetallic oxides as shown in Table 2.

3. Results and discussion

The synthesis of bimetallic alkoxides was confirmed with the help of quantitative yield of the product and as well as quantitative yield of KCl. The formation of these alkoxides was further confirmed with the help of microanalysis of C and H, IR and ^{1}H NMR studies. When freshly prepared they are extremely susceptible to moisture to form the hydrated oxides. All bimetallic alkoxides were soluble in mother liquor and thermally labile but could not be distilled or sublimed at 200 °C/10^{-3} torr. Elemental analyses were performed under ambient conditions; a partial hydrolysis is unavoidable and invariably associated with the handling procedure. The analytical data of alkoxides and their corresponding oxides as shown in Table 3 support the formation of the product.

The metal alkoxides and their corresponding metal oxides were characterized with the help of FT-IR by observing the main characteristic absorption peaks as shown in Table 4. The absence of ν_{C-O} bands (terminal and bridging) in corresponding metal oxides clearly supports the formation of oxides from their corresponding bimetallic alkoxides. The significant down field shift was observed in metal oxides for the absorption band of ν_{M-O} (asymm), ν_{Ce-O} (asymm), ν_{M-O} (symm) due to M–O stretching bond.

A UV absorption edge was found to be very sensitive with a change in band gap and the coordination around the central metal ion. The absorptions of UV–visible spectra of the alkoxides can be attributed to the CT band of unshared electron pairs on the oxygen atoms to the empty Ce^{3+} metal orbital. The sharpness of the absorption band shows the presence of 4f electrons of Ce^{3+}. Ce^{3+} was found to be suitable for the studying changes within the coordination number and oxygen donor properties of the ligands (Westin et al., 1998; Yatsimirskii and Davidenko, 1979). The CT bands of all three metal alkoxides was found to be due to the presence of the Ce^{3+} ion. The fine structural peak in isopropanol is virtually unchanged due to a weak interaction with the solvent. In solution these alkoxides does not show any ageing effect for many days in dry atmosphere. UV spectra are shown in Fig. 1.

^{1}H NMR spectra give useful structural information of the precursor. Although no suitable crystals for X-ray studies were

Table 1 Millimoles ratio, yield and nature of metal alkoxide.

$KM(OPr^i)_5$ g (mmol)	$CeCl_3$ g (mmol)	Weight of the compounds in g observed (calc)	Weight of KCl in g observed (calc)	Nature of the compounds
1.63 (4.26)	0.35 (1.42)	1.66 (1.72)	0.32 (0.40)	White liquid
1.39 (3.07) M = Ti and Sn	0.25 (1.02)	1.41 (1.42)	0.23 (0.25)	White viscous liquid

Table 2 Millimoles ratio, yield and nature of metal oxide.

$CeCl_3$ g (mmol)	Double alkoxides g (mmol)	Weight of the metal oxides in g observed (calc)	Nature of the metal oxides
0.89 (3.61)	$[Ce\{Sn(OPr^i)_5\}_3]$ 1.0 (0.72)	1.04 (1.07)	Light brown solid
1.05 (4.26)	$[Ce\{Ti(OPr^i)_5\}_3]$ 1.02 (0.86)	1.05 (1.17)	Orange solid

Table 3 Elemental analysis.

	Compounds	OPr^i obtained (calc)	Ce obtained (calc)	Sb/Ti/Sn obtained (calc)
1	$[Ce\{Sb(OPr^i)_4\}_3]$	57.62 (58.30)	11.24 (11.57)	29.79 (30.07)
	$[Ce_5Sb_3O_{12}]$	–	55.44 (55.69)	28.94 (29.04)
2	$[Ce\{Ti(OPr^i)_5\}_3]$	75.47 (75.73)	11.57 (11.99)	11.82 (12.29)
	$[Ce_6Ti_3O_{15}]$	–	67.93 (68.67)	11.28 (11.73)
3	$[Ce\{Sn(OPr^i)_5\}_3]$	63.86 (64.08)	9.93 (10.14)	25.56 (25.78)
	$[Ce_6Sn_3O_{15}]$	–	58.16 (58.51)	24.58 (24.79)

Table 4 FT-IR data for metal alkoxide and metal oxide.

	Compounds	$\nu_{Ce-O(asym)}$	$\nu_{M-O(asym)}$	$\nu_{Ce-O(sym)}$	$\nu_{M-O(sym)}$	$\nu_{C-O(asym\ +\ sym)}$
1	$[Ce\{Sb(OPr^i)_4\}_3]$	1627w	1382.6vs	1135.1vs	1167.6s	819.7 and 852.5br
	$[Ce_5Sb_3O_{12}]$	1637.4vs	1439w	1020.8m	1096.7br	–
2	$[Ce\{Ti(OPr^i)_5\}_3]$	1633br	1376s	1130.9s	1163.5s	819.1 and 848.5br
	$[Ce_6Ti_3O_{15}]$	1634.8vs	1464.3m	1101.8m	1125.3m	–
3	$[Ce\{Sn(OPr^i)_5\}_3]$	1636.4w	1377.9s	1131.2s	1162.7s	817.3 and 847.9m
	$[Ce_6Sn_3O_{15}]$	1635.8s	1456.7m no significant peak were absorbed			

Vs = very strong, s = strong, m = medium, w = weak, vw = very weak, br = broad.

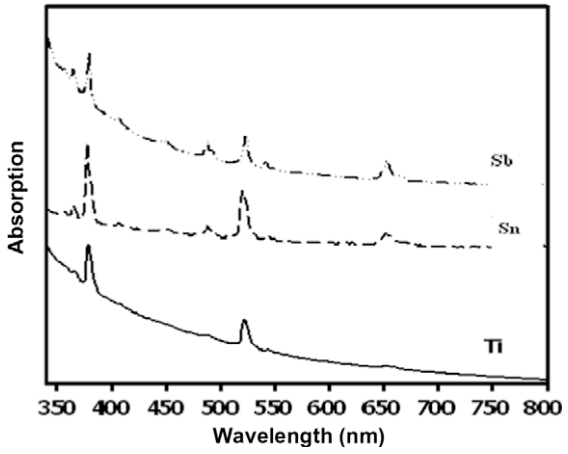

Figure 1 UV–vis spectra for obtained complexes.

Table 5 ^1H spectral data (δ/ppm) for the complexes.

Compounds	CH_3	CH solvent
$[Ce\{Sb(OPr^i)_4\}_3]$	1.20 (br)	3.96 (br) C_6D_6
$[Ce\{Ti(OPr^i)_5\}_3]$	1.23 (br)	4.45 (br) C_6D_6
$[Ce\{Sn(OPr^i)_5\}_3]$	1.15(br)	4.30 (br) $CDCl_3$

Table 6 C and H analysis.

Compounds	C observed (calc)	H observed (calc)
$[Ce\{Sb(OPr^i)_4\}_3]$	34.81 (35.57)	5. 96 (6.92)
$[Ce\{Ti(OPr^i)_5\}_3]$	45.49 (46.20)	8.51 (8.98)
$[Ce\{Sn(OPr^i)_5\}_3]$	38.78 (39.09)	7.08 (7.60)

obtained due to hydrolytic instability. ^1H NMR ($CDCl_3$ or C_6D_6) spectra were carried out and exhibits two types resonance peaks for isopropyl protons with correct integration ratio, but the peaks are not sharp due to the para magnetic behavior. The significant ^1H peaks are given in Table 5. Absence of ^1H NMR signal and the microanalysis support the formation of metal oxide.

Table 7 Mass spectrum with important fragmentation peaks.

Compounds	Ce_2O_3 I, m/z^+	$Sb_2O_3/SnO_2/TiO_2$ I, m/z^+	Ce $(OPr^i)_3$ I, m/z^+	$Sn(OPr^i)_4/Ti(OPr^i)_4/Sb(OPr^i)_3$ I, m/z^+
$[Ce\{Sb(OPr^i)_4\}_3]$	15, 328	15, 291	16, 317	47, 299
$[Ce_5Sb_3O_{12}]$	20, 328	32, 291	–	–
$[Ce\{Sn(OPr^i)_5\}_3]$	20, 328	25, 150.7	12, 317	33, 355
$[Ce_6Sn_3O_{15}]$	25, 328	20, 150.7	–	–
$[Ce\{Ti(OPr^i)_5\}_3]$	30, 328	40, 80	47, 317	27, 299
$[Ce_6Ti_3O_{15}]$	30, 328	30, 80	–	–

The formation of bimetallic oxides was further confirmed by X-ray energy dispersive spectroscopy (EDS) micro elemental analysis as shown in Table 6. The mass spectra do not give any conclusive evidence for the formation of heterometallic molecules in gas phase probably due to the breakdown of the compounds under the high vacuum used in mass spectrometer. The limited characteristic fragments ion peak of low intensity has been observed in standard electron impact conditions, which corresponds to simple decomposed metal oxides. The important fragmentation ion peaks are given in Table 7.

The thermal behavior of metal oxides was investigated by thermogravimetry (TG) and differential thermal analysis (DTA) as shown in Fig. 2. The thermal decomposition of oxides may be described as a stepwise process. The first weight loss occurs below 200 °C and is attributed to the removal of solvent trapped in oxides. Prominent exothermic peaks around 190 °C can be attributed to the removal of organic residues.

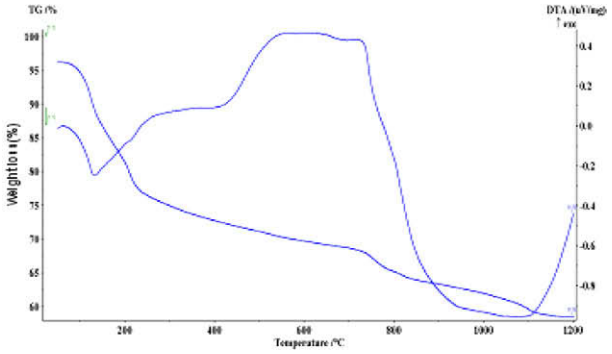

$[Ce_5Sb_3O_{12}]$

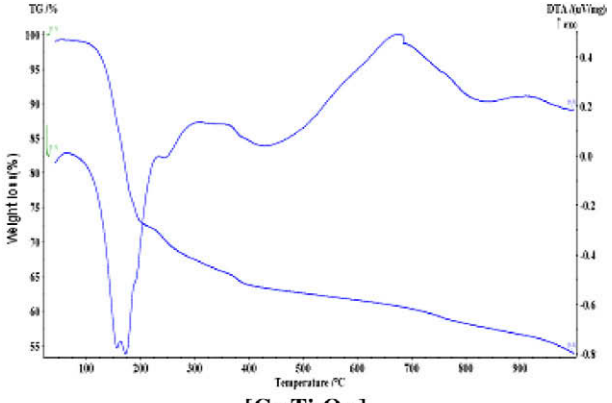

$[Ce_6Ti_3O_{15}]$

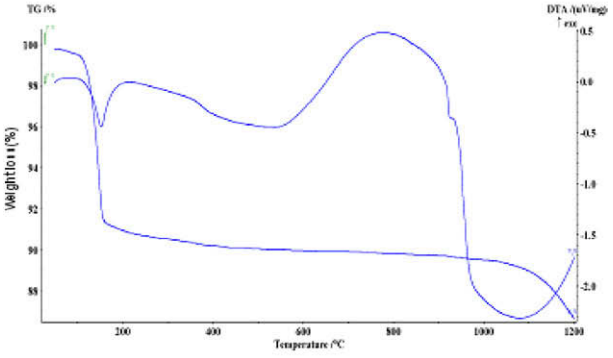

$[Ce_6Sn_3O_{15}]$

Figure 2 TG data showing the weight loss expressed as a percentage of weight as a function of temperature. The heating rate was 10 °C/min in argon atmosphere. DTA data shows exothermic peaks.

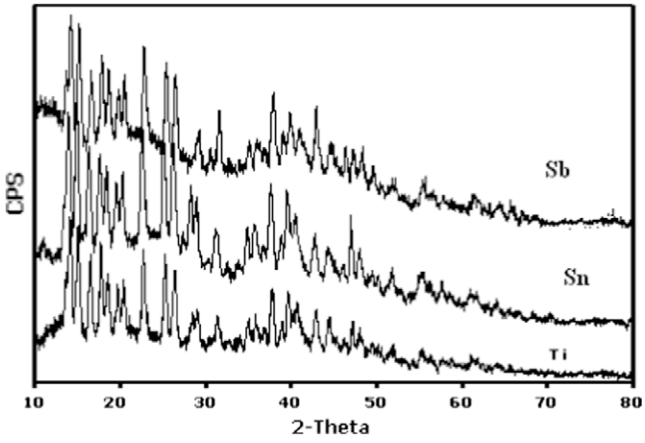

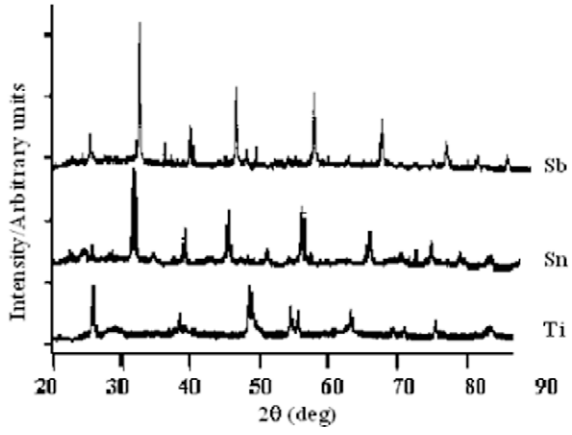

Figure 3 XRD diffraction patterns describe the nature of the compounds at room temperature and after calcinations.

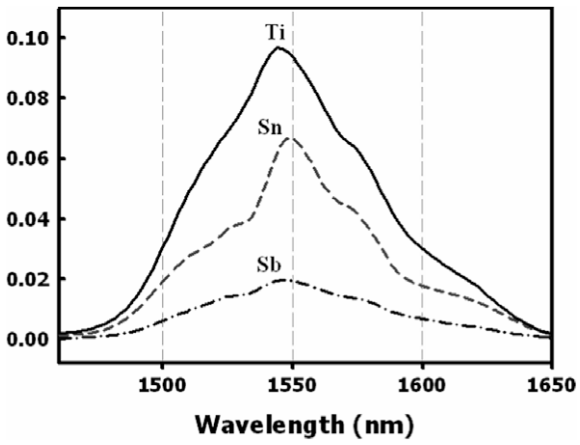

Figure 4 Photoluminescence profiles for complexes.

Little mass loss was noticed below 600 °C, thus support the formation of an oxide with a definite chemical composition after the removal of impurities. The exothermic peaks located at 800–850 °C supports the formation of a well-organized metal oxide network after the decomposition of inorganic residue (Alves et al., 2008).

The purity of bimetallic oxide was ascertained by powder X-ray diffraction and compared with standard diffraction data files (JCPDS). The XRD patterns shows broad diffraction peak due to their poor crystallinity at room temperature. The same diffraction patterns were observed for other metal oxides at room temperature probably due to similar type of molecular structures (Andrianainarivelo et al., 1997). X-ray diffraction peaks as shown in Fig. 3 exhibits sharp patterns on calcinations supporting the degree of crystallinity with metal–oxygen framework with the removal of impurities. The size of the particles was about 5–10 nm as calculated by using the Scherer equation (Cullity, 1967).

Luminescence spectra of homogenous metal oxides as shown in Fig. 4 supports fact the excitation between $\pi \rightarrow \pi^*$ transition gives a characteristic $^5D_0 \rightarrow {}^7F^g$ emission. This indicates fast intermolecular energy transfer from oxygen to the central metal ion. The broad emission at around 1550 nm extending from 1500 to 1600 nm was observed and is attributed to $\pi \rightarrow \pi^*$ transitions. The spectral half width of the emission band from the maximum is about 50 nm and it is due to heterogeneous nature and Stark splitting of the excited and ground states. The broad spectrum helps for the fabrication of potential optical amplifiers depending on the nature of the precursor chemistry. It is concluded that the luminescent

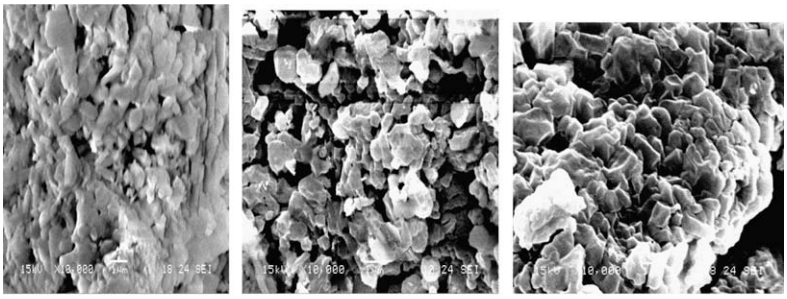

Figure 5 SEM shows surface morphologies at room temperature.

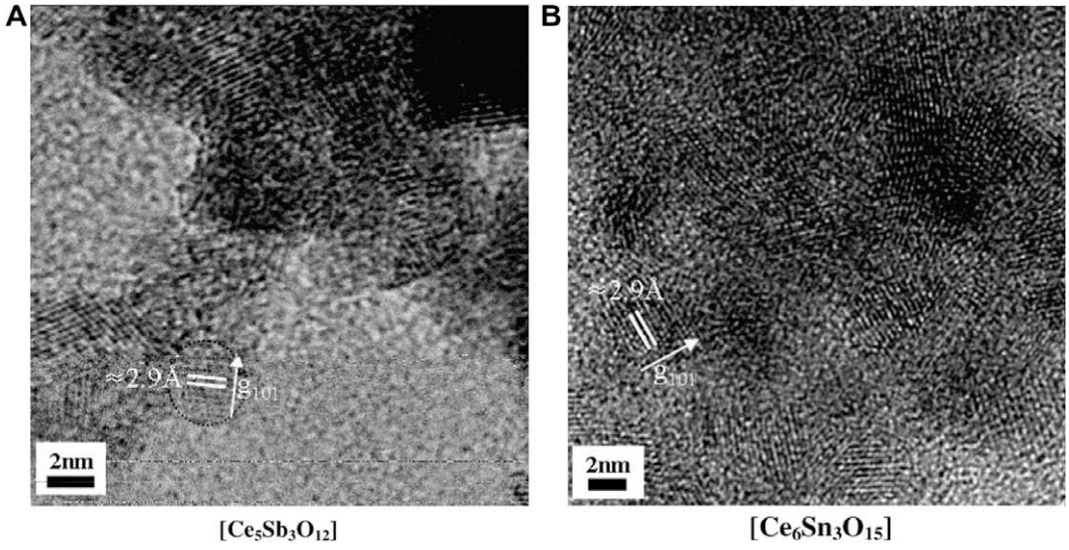

Figure 6 TEM images of the particles at room temperature.

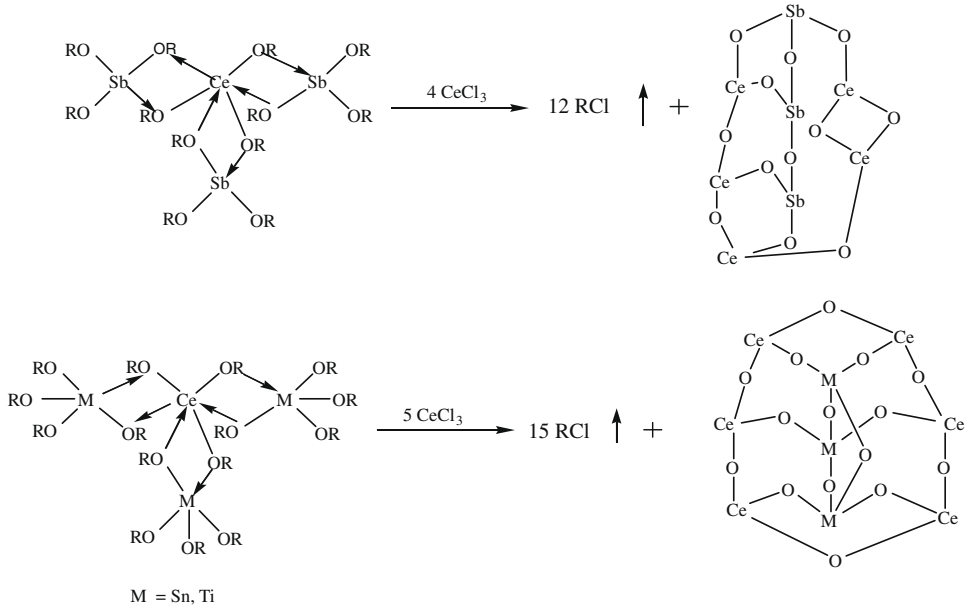

Figure 7 Structure proposed based on using the imaging systems for the characterizations of the obtained products.

properties depend on the metal oxide morphology, particles size, its distribution and the methodology (Riwotzki and Haase, 1998; Riwotzki et al., 1998).

SEM shows dense structure with unfaceted pores surface with the oxides grain to be micrometer-sized, which build up to form many tiny particles with the polydispersed nature without any observable defects in particle size and shape as shown in Fig. 5. Therefore, it is concluded that the nature of the metal oxides strongly depends on the chemical composition of the metal alkoxides as a molecular precursor and the methodology used for particles synthesis.

TEM shows (Fig. 6) that the size of particles was about 5–10 nm in heterometallic oxide which agrees well with XRD determinations using the Scherer equation. Moreover the metal oxide nanopowder has slight an agglomeration due to the presence of their surface energy based on Ostwald ripening process. However dispersibility of particles is related to the role of the dispersing agent and synthetic methodology (Hyeon, 2007; Lee et al., 2006). Though there was considerable distribution in size, redispersed nanocrystal obtained from low concentration reactions appeared isolated or only very loosely aggregated depending on TEM sample preparation. Many particles exhibited irregular shapes with high crystalline in nature. On the basis of above studies, the following plausible structures can be suggested for molecular precursor and their corresponding metal oxides as shown in Fig. 7.

4. Conclusion

The design of molecular routes for solid metal oxides with functional properties has become an important area due to their technological importance. Physical properties of the final metal oxides can be controlled at the molecular level by using single source molecular precursor at low temperature via soft chemistry approach. The physico-chemical property of molecular precursor plays a key role in controlling the high compositional purity in the final products. Aging has a significant effect on the texture and the structure of the mixed oxide. However, the research is still underway to find new chemical routes without sophisticated procedure to obtain homogenous and ultra fine multicomponent materials without agglomeration for high tech application in green conditions.

Acknowledgement

The author is gratefully indebted to Mrs. D. Paravati for the technical assistance.

References

Alves, V.A., Da Silva, L.A., Coleta, J.F.B., 2008. Quim. Nova 23, 608.
Andrianainarivelo, M., Corriu, R.J.P., Leclercq, D., Mutin, P.H., Vioux, A., 1997. J. Sol–Gel Sci. Technol. 8, 89.
Backov, R., 2006. Soft Matter 2, 452.
Bradley, D.C., Mehrotra, R.C., Gaur, D.C. (Eds.), 1978. Metal Alkoxides. Academic Press, London.
Bradley, D.C., Mehrotra, R.C., Roth Well, I.P., Singh, A. (Eds.), 2001. Alkoxo and Aryloxo Derivatives of Metals. Academic Press Inc., San Diego, CA.
Brinker, C.J., Clark, D.E., Ulrich, D.R., 1984. Better Ceramics through Chemistry. Elsevier, New York.
Cullity, B.D., 1967. Elements of X-ray Diffraction. Addison-Wesley, Massachussetts, p. 262.
Hyeon, T.J., 2007. J. Am. Chem. 129, 5812.
Jolivet, J.P., 2000. Metal Oxide Chemistry and Synthesis, From Solution to Solid State. Wiley, Chichester.
Kessler, V.G., 2003. Chem. Commun., 1213.
Klabunde, K.J. (Ed.), 2000. Nanoscale Materials in Chemistry. Wiley-Interscience, New York.
Lee, T.H., Kim, J.H., Bae, B.S., 2006. J. Mater. Chem. 16, 1657.
Mehrotra, R.C., 1954. J. Ind. Chem. Soc. 81, 904.
Mehrotra, R.C., 1992. In: Reisfeld, R., Jorgensen, C.K. (Eds.), Chemistry, Spectroscopy and Applications of Sol–gel Glasses. Springer-Verlag, Berlin, Heidelberg.
Riwotzki, K., Haase, M., 1998. J. Phys. Chem. B 102, 10129.
Riwotzki, K., Meyssamy, H., Kornowski, A., Haase, M., 1998. J. Phys. Chem. B 104, 2824.

Sapra, S., Sarma, D.D., 2004. In: Rao, C.N.R., Muller, A., Cheetham, A.K. (Eds.), The Chemistry of Nanomaterials, Synthesis, Properties and Applications. Wiley, VCH, Weinheim.

Trevor, D.T., Sakka, S. (Eds.), 2004. Hand Book of Sol–Gel Science and Technology Processing Characterization and Applications. Kluwer Academic Publishers, Norwell, USA.

Turova, N.Ya., Turevskaya, E.P., Kessler, V.G., Yanovskaya, A.I. (Eds.), 2002. The Chemistry of Metal Alkoxides. Kluwer Academic Publishers, London.

Vogel, A.I., 1989. Textbook of Quantitative Analysis, fifth ed. Longman.

Westin, G., Norrestam, R., Nygren, M., Wijk, M., 1998. J. Solid State Chem. 135, 149.

Yatsimirskii, K.B., Davidenko, N.K., 1979. Coord. Chem. Rev. 27, 223.